Bollettino di Geofisica Teorica ed Applicata Vol. 52, n. 2, pp. x-xx; June 2011
DOI 10.4430/bgta0008

Conditions for crust and tube formation in lava flows with power-law rheology

M. Filippucci[1], A. Tallarico[2] and M. Dragoni[3]

[1] *Istituto Nazionale di Geofisica e Vulcanologia, Catania, Italy*
[2] *Dipartimento di Geologia e Geofisica, Università di Bari, Italy*
[3] *Dipartimento di Fisica, Università di Bologna, Italy*

(Received: March 29, 2010; accepted: July 20, 2010)

ABSTRACT We studied the conditions of crust and tube formation of a lava flow moving under the effect of gravity in a rectangular cross-section channel and assumed a power-law rheology for lava. We followed the work of Valerio *et al.* (2008), who studied the effect of surface cooling on the formation and accretion of the crust in the central region of the channel, assuming for lava a Newtonian rheology. According to these authors, tube formation is influenced by topography and channel morphology. In this work, we extended this study to a non-Newtonian rheology, in particular to the power-law rheology. Results indicate that a power-law rheology strongly influences the condition of crust formation but does not produce significant differences as a function of topographical or morphological variations.

Key words: power law rheology, crust formation, channel flow.

1. Introduction

Many observed basaltic lava channels exhibit a surface crust that is carried along by the flow and looks dark due to its lower radiative temperature (Griffiths *et al.*, 2003). When the crust is thick enough so as to form a connected roof, a lava tube can arise (Peterson *et al.*, 1994). Models of lava tube formation, as a consequence of the crust welding to the channel levées , have been proposed considering lava as a Bingham liquid (Dragoni *et al.*, 1995) or a Newtonian liquid (Cashman *et al.*, 2006). Valerio *et al.* (2008) described the formation of the surface crust as a consequence of the surface cooling of a Newtonian lava flow by introducing a temperature-dependent, yield strength, which models the plastic behavior of lava under the solidus temperature. The authors also explored how variations in channel width, ground slope and volume flow rate can affect the formation of a lava tube.

Laboratory studies on basaltic melts have recently shown that lava rheology can exhibit a non-Newtonian behavior under certain conditions which include vesicularity (Spera *et al.*, 1988; Badgassarov and Pinkerton, 2004), crystal concentration (Pinkerton and Stevenson, 1992; Smith, 2000; Sonder *et al.*, 2006; Champallier *et al.*, 2008), temperature and shear rates (Shaw *et al.*, 1968).

There is general consensus that the viscosity of magma has a non-Newtonian pseudoplastic behavior, with the only exception of Smith (2000), who attributes a dilatant rheology to lava at high crystal concentrations. Pseudoplasticity and dilatancy belong to a power law rheology, where

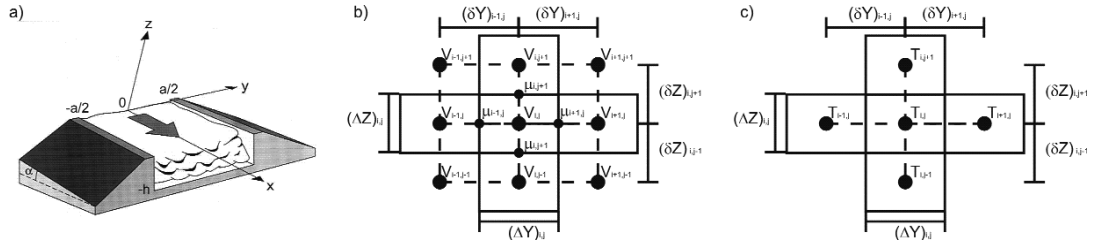

Fig. 1 - Coordinate system (a); computational molecule for the dynamical problem (b); computation molecule for the thermal problem (c).

the apparent viscosity depends on a power of the strain rate with exponent *n.* If *n* is lower than 1, the fluid is pseudoplastic and it thins with an increase of shear stress. If *n* is greater than 1, the fluid is dilatant and it thickens with an increase of shear stress.

When solving the problem of a gravity-driven lava flow, the power-law rheology introduces a non-linearity in the diffusion term of the momentum equation and an analytical solution of the governing differential equations is not possible. This has given rise to various approximate solutions to the problem. The fully developed laminar flow of power-law fluids has been studied numerically using the finite element method (Syrjälä, 1995) and the finite volume method (Capobianchi, 2008) for a pressure driven flow in a horizontal rectangular duct and using the finite volume method for a gravity driven flow down an inclined rectangular duct (Filippucci *et al.*, 2010).

In this work, we analyzed the crust and tube formation by assuming a power-law rheology and investigated the difference with respect to the model of Valerio *et al.* (2008).

2. Model equations

We consider a viscous fluid flowing in the x direction down an inclined rectangular channel, with the cross-section parallel to the yz plane. The width of the channel is a and the thickness is h; the slope of the inclined plane is α. The channel and the coordinate system are shown in Fig. 1a. The flow is assumed steady, laminar and subjected to the gravity force. The fluid is assumed isotropic and incompressible, with constant density ρ.

Cooling is described for a lava flow exiting from a vent with an effusion temperature T_0=1273 K.

We assume the flow as laterally isothermal (the effects of levées and of the ground on cooling are neglected) and the cooling process occurs from the upper surface by assuming a fixed value of the heat flux $q_0=10^4$ W·m^{-2} where q_0 can be considered as representative of the sum of the main contributions to surface cooling (radiation and forced convection). It describes the average heat loss from the surface that is covered by solid crust and from the crust-free shear regions (Valerio

et al., 2008).

The momentum and energy equations governing the fluid flow and heat transfer are the following:

$$\rho g_x = \frac{\partial}{\partial y}\left(\eta_{app}\frac{\partial v_x}{\partial y}\right)+\frac{\partial}{\partial z}\left(\eta_{app}\frac{\partial v_x}{\partial z}\right)=0 \tag{1}$$

$$\frac{\partial T}{\partial t}=\chi\left(\frac{\partial^2 T}{\partial y^2}+\frac{\partial^2 T}{\partial z^2}\right) \tag{2}$$

where v_x and g_x are the x components of velocity and acceleration of gravity respectively, T is the temperature, η_{app} is the apparent viscosity, χ is the thermal diffusivity

$$\chi=\frac{K}{\rho c_p} \tag{3}$$

where K is the thermal conductivity and c_p is the heat capacity.

The apparent viscosity of a power-law fluid, under our assumptions, is:

$$\eta_{app}=k\left[\left(\frac{\partial v_x}{\partial y}\right)^2+\left(\frac{\partial v_x}{\partial z}\right)^2\right]^{\frac{n-1}{2}} \tag{4}$$

where k is the fluid consistency, which is a measure of the resistance to shear.

The boundary conditions are the no-slip and the adiabatic condition at the walls and the constant heat flux at the upper surface. Initially, the fluid has a uniform temperature T_0. The dynamic boundary conditions are:

$$\frac{\partial v_x}{\partial y}(0,z)=0;\ \frac{\partial v_x}{\partial z}(y,0)=0 \tag{5}$$

$$v_x(y,-h)=0;\ v_x\left(\pm\frac{a}{2},z\right)=0 \tag{6}$$

At the time t=0, a constant heat flux q_0 is set and the thermal boundary conditions for t>0 become:

$$\frac{\partial T}{\partial y}(0,z)=0;\ \frac{\partial T}{\partial z}(y,0)=-\frac{q_0}{K} \tag{7}$$

$$\frac{\partial T}{\partial y}(\pm\frac{a}{2},z)=0;\ \frac{\partial T}{\partial z}(y,-h)=0 \tag{8}$$

The dynamic problem is solved numerically by using the control volume method with an iterative solver (Filippucci *et al.*, 2010). In summary, the calculation domain is divided into a finite number of non-overlapping sub-domains (or control volumes CV). Variables are arranged with the computational node located at the center of an internal CV. The CV at the boundary is half of the internal CV and the computational node is a boundary node. The position of any CV is identified by a set of two indices (*i,j*) as shown in Fig. 1b.

The differential equation is integrated over each CV using linear interpolation functions between the two nearest grid points. This is a second-order approximation scheme which corresponds to the Central-Difference approximation of the first derivative in the Finite Difference methods (Ferziger and Peric, 2002). This is known as discretization procedure and finds an algebraic equation that is solved numerically and represents an approximation of the analytical solution.

The discretized momentum equation in grid notation is the following:

$$V_{i,j}=\frac{1}{a_{i,j}}\left[a_{i-1,j}V_{i-1,j}+a_{i+1,j}V_{i+1,j}+a_{i,j-1}V_{i,j-1}+a_{i,j+1}V_{i,j+1}+b\right] \tag{9}$$

where

$$a_{i,j}=a_{i-1,j}+a_{i+1,j}+a_{i,j-1}+a_{i,j+1}. \tag{10}$$

Focusing on $a_{\mathrm{i\text{-}1,j}}$ and considering that the coefficients on the other faces are treated in the same way, we have:

$$a_{i-1,j}=\frac{\eta_{i-1,j}\Delta Z_{i,j}}{(\delta Y)_{i-1,j}} \tag{11}$$

and

$$b=\rho g_x \Delta Y_{i,j}\Delta Z_{i,j}. \tag{12}$$

For a more complete treatment of the discretization of the viscosity coefficient $\eta_{\mathrm{i\text{-}1,j}}$ in Eq.

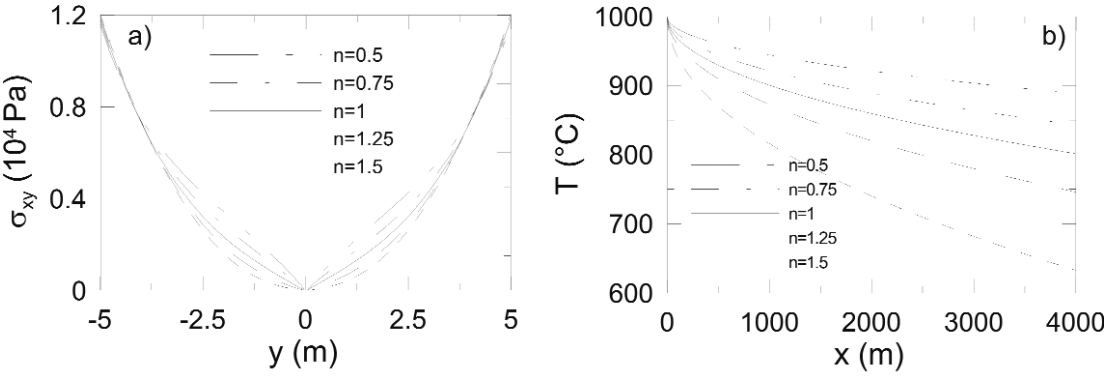

Fig. 2 - a) Shear stress profiles σ_{xy}^{M} (y, 0) for different values of n (a=10 m, h=3 m, α=0.2 rad, ρ=2800 kg m^{-3}, k=10^4 *Pa* s^n); b) surface temperature T as a function of x for different values of n (c_p=837 J kg^{-1} K^{-1}, K=3 W K^{-1} m^{-1}, q_0=10^4 W m^{-2}).

(11), the reader should refer to Filippucci *et al.* (2010).

From the solution for the velocity, we can compute the shear stress as:

$$\sigma_{xy} = \eta_{app} \frac{\partial v_x}{\partial y}. \tag{13}$$

Fig. 2a shows σ_{xy} profiles in z =0 for different values of n.

The discretization of the energy equation involves, in addition, the integration of Eq. (2) over the time interval from t to $t+\Delta t$. The integration is operated by using a fully implicit scheme, which ensures simplicity and physical consistency (Patankar, 1980). The value T^0 at the time t is used to find the value T at the time $t+\Delta t$. The superscipt ^{0} denotes the value of T at the preceding time step.

The discretized energy equation in grid notation is:

$$T_{i,j} = \frac{1}{c_{i,j}}\left[c_{i-1,j}T_{i-1,j} + c_{i+1,j}T_{i+1,j} + c_{i,j-1}T_{i,j-1} + c_{i,j+1}T_{i,j+1} + d \right] \tag{14}$$

where

$$c_{i,j} = c_{i-1,j} + c_{i+1,j} + c_{i,j-1} + c_{i,j+1} + c_{i,j}^0 \tag{15}$$

and

$$c_{i,j}^0 = \rho c_p \frac{\Delta Y_{i,j} \Delta Z_{i,j}}{\Delta t} \tag{16}$$

$$d = c_{i,j}^0 T_{i,j}^0. \tag{17}$$

Focusing on $c_{i-1,j}$ and considering that the coefficients on the other faces are treated in the same way, we have:

$$c_{i-1,j} = \frac{\chi \Delta Z_{i,j}}{(\delta Y)_{i-1,j}}. \tag{18}$$

The computational molecule of the thermal problem at the time t is shown in Fig. 1c.

In our problem, the velocity field is independent of the temperature field and it is solved first. Once the velocity field is known, the temperature field can be solved.

The algebraic Eqs. (9) and (14) are solved iteratively using a classical point by point Gauss-Seidel method. Although the use of an iterative solver is necessary only for the momentum equation (Ferziger and Peric, 2002), we adopted the same solution procedure also for the energy equation.

Valerio *et al.* (2008) substituted the time dependence of the solution in T with a space dependence by the relation:

$$t = \frac{x}{\overline{v_x}(z)} \tag{19}$$

where

$$\overline{V_x}(z) = \frac{1}{a} \int_{-\frac{a}{2}}^{\frac{a}{2}} V_x(y,z) dy \tag{20}$$

Lava velocity is strongly influenced by the exponent n of the power-law rheology. Fig. 2b shows surface cooling as a function of the distance x from the vent, for different values of n.

3. Crust formation

To model the plastic behavior of the lava crust, Valerio *et al.* (2008) introduced a temperature-dependent yield strength τ, given by:

$$\tau = \tau_0 \left[1 - e^{\left(\frac{T}{T_s} - 1 \right) b} \right], T \le T_s \tag{21a}$$

$$\tau = 0, \; T \ge T_s \tag{21b}$$

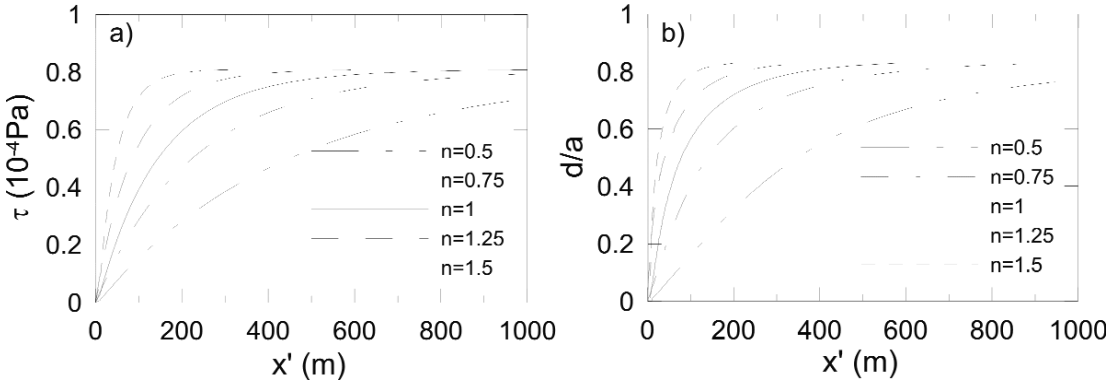

Fig. 3 - a) Yield strength τ as function of x' for different value of n; b) crust coverage on lava surface d/a as function of x' for different values of n (a=10 m, h=3 m, α=0.2 rad, ρ=2800 kg m^{-3}, k=10^4 Pa s^n).

where T_s is the solidus temperature. τ_0 is the maximum yield strength (set equal to 8100 Pa); b is a constant (set equal to 170).

In Fig. 3a, we plotted τ as a function of x', for different values of n, where x' is a spatial variable which vanishes where the lava surface reaches the solidus temperature T_s=1173 K.

In the regions of the lava surface where the horizontal shear stress $\sigma_{xy}<\tau$, crust formation and growth are possible; where $\sigma_{xy}>\tau$ shearing movements occur and crust formation is inhibited. d/a is the portion of the crust surface covered by the crust and Fig. 3b shows d/a as a function of x', for different values of n.

4. Tube formation

In the example of Fig. 3b, the crust grows up to a maximum value d/a=0.83, meaning that the crust never entirely covers the lava surface if we simply consider the cooling effect. This is valid for every value of n we used in the power law rheology. Finally, we analyze how changes in the channel width a, channel slope α and lava flow rate q can modify d/a so as to reach the condition for tube formation, d/a=1.

First, we analyzed the trend of the maximum shear stress, $\sigma_{xy}^M = \sigma_{xy}(\pm a/2.0)$ as a function of the channel half width a/2 for two different values of the slope α (Figs. 4a and 4b).

Then, we computed d/a as a function of a/2, by comparing σ_{xy}^M with τ_0. For this example, we considered four values of the exponent n=0.5, 0.75, 1.25, 1.5 and two values of the ground slope α=0.2 and 0.4 rad. Results are in Figs. 4c and 4d. In each plot, the comparison with the Newtonian case is also presented (n=1).

As a second effect, we studied the variation of σ_{xy}^M as a function of the channel slope α for two different values of width a=10 and 20 m and by varying the rheology as before (Figs. 5a and 5b). The ratio d/a as a function of α, for the two values of a, by varying the rheology is plotted and compared with the Newtonian case (Figs. 5c and 5d). As we expected, the curve corresponding to the Newtonian case lies exactly between the pseudoplastic and the dilatant cases.

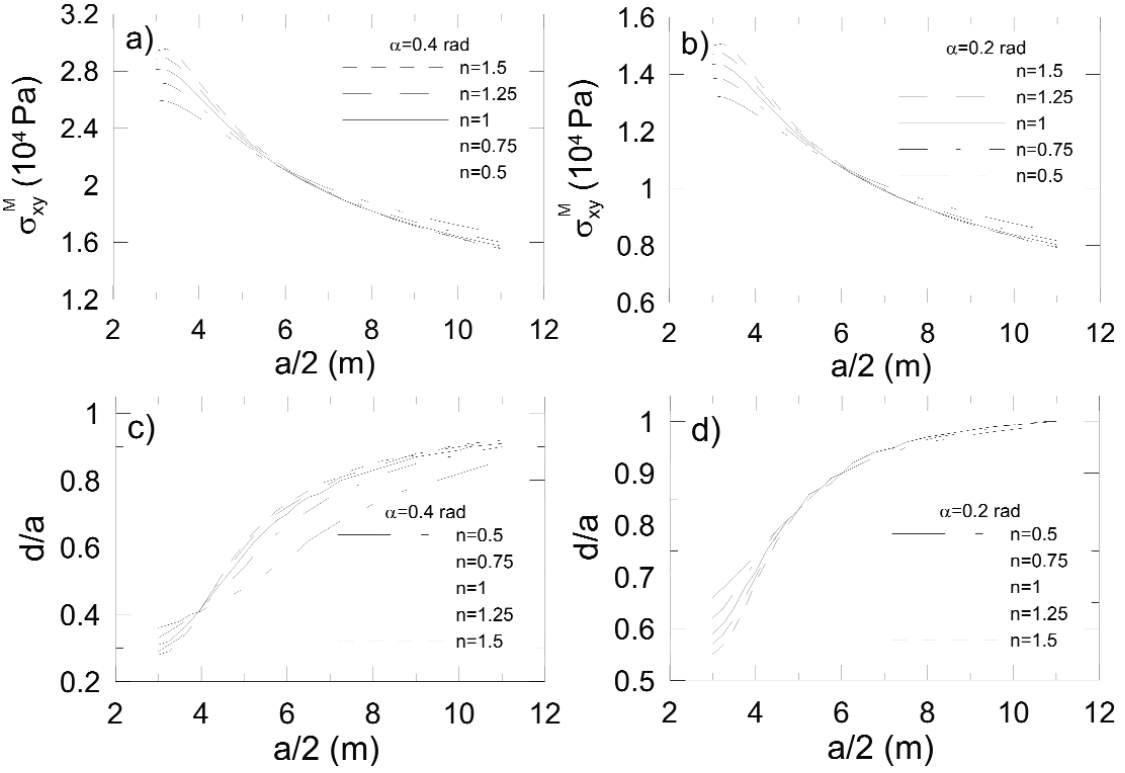

Fig. 4 - σ^M_{xy} as function of *a/2* (*h*=3 m, ρ=2800 kg m^{-3}, *k*=10^4 Pa s^n) for α=0.4 rad (a) and α=0.2 rad (b); *d/a* as function of a/2 for α=0.4 rad (c) and α=0.2 rad (d).

Finally, we analyzed the variation of σ^M_{xy} with the volume flow rate *q* for two different ground slopes α=0.2 and 0.4 rad (Figs. 6a and 6b), by varying *n*. In Figs. 6c and 6d we plotted *d/a* as a function of *q*, for the two slopes and for different values of *n*.

5. Discussion and conclusion

In a previous paper (Filippucci *et al.*, 2010), we showed that the velocity profiles of a gravity-driven channeled lava flow with a Newtonian rheology can be strongly modified by the assumption of a power-law rheology. In particular, it was shown that differences among Newtonian, pseudoplastic and dilatant rheologies grow by increasing the channel slope.

In this paper, we extended the study of the differences between the Newtonian and the power-law model. We used the model published by Valerio *et al.* (2008) to study how the power-law rheology can affect the conditions of crust and tube formation for a gravity-driven, channeled lava flow. To facilitate the comparison with the Newtonian case of Valerio *et al.* (2008), we used the same values of model parameters τ_0, *b*, ρ, *h*, *a*, α, *g* and we used the value of η to model *k*.

First, we studied the surface cooling of the lava channel by numerically solving the heat

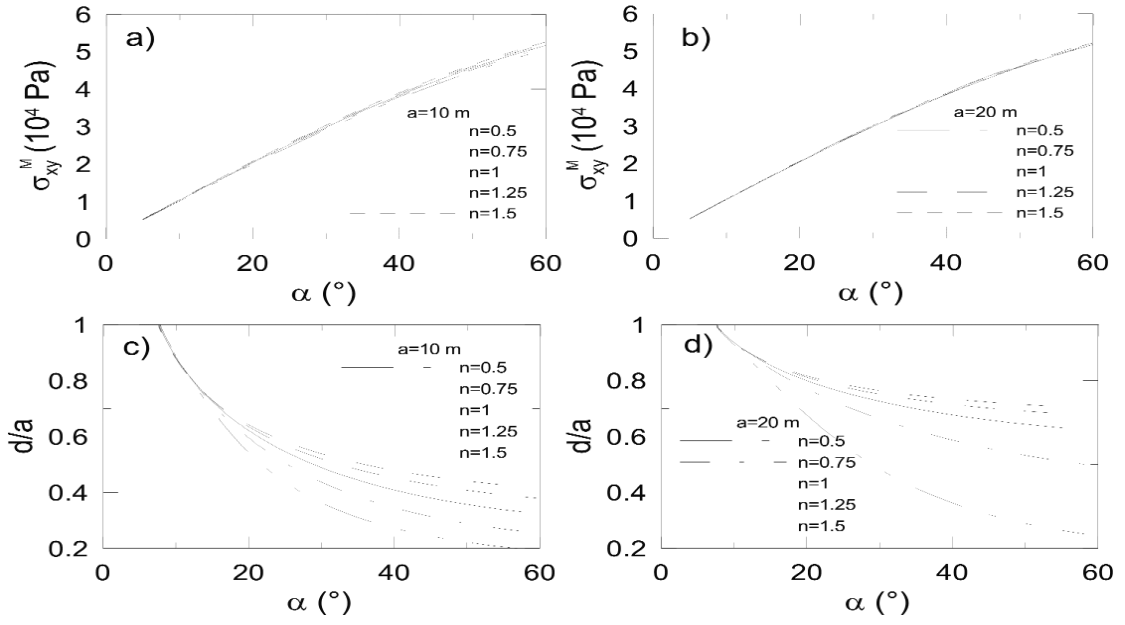

Fig. 5 - σ_{xy}^{M} as function of channel slope α (h=3 m, ρ=2800 kg m^{-3}, k=10^4 Pa s^n) for a = 10 m (a) and a = 20 m (b); d/a as function of α for a = 10 m (c) and a = 20 m (d).

conduction equation.

We can observe that for the dilatant fluid (n=1.25 - 1.5) the solidus is reached much closer to the vent than for the Newtonian fluid (n=1) and for the pseudoplastic fluid (n=0.75-0.5).

As the surface temperature reaches T_s (x'=0), τ starts to increase up to the threshold τ_0 and the distance from the vent where τ reaches τ_0 strongly depends on the assumption on rheology (Fig. 3a). When τ increases, the crust width d/a grows too and attains its maximum width and stops widening where τ reaches τ_0 (Fig. 3b). In particular, with respect to the Newtonian fluid, while for the dilatant fluid the crust stops widening very close to the point where T=T_s, the pseudoplastic fluid will cover a much longer distance before the crust reaches its maximum width. This result is a consequence of the substitution (19). In fact, with our assumptions, the pseudoplastic fluid down a slope flows with $\bar{v}_x$ greater than that of the Newtonian fluid, which in turn is greater than that of the dilatant fluid, and this has the consequence that, at the same time as t, it will have covered the greatest distance x before the crust stops widening.

The transition from a mobile crust to a solid roof is achieved when d/a=1. We also explored the possibility of developing a solid roof and analyzed the effect of the non-linear rheology. Following Valerio *et al.* (2008), we studied the effects of variations of topography (slope) and of morphology (width and volume flow rate) of the lava channel on σ_{xy}^{M} and on d/a. We considered four different values of n (n=0.5, 0.75, 1.25, 1.5) and compared our results with the Newtonian rheology. We found that, independently of n, σ_{xy}^{M} and d/a are decreasing functions of channel width (Fig. 4) and are increasing functions of channel slope (Fig. 5) and of volume flow rate (Fig.

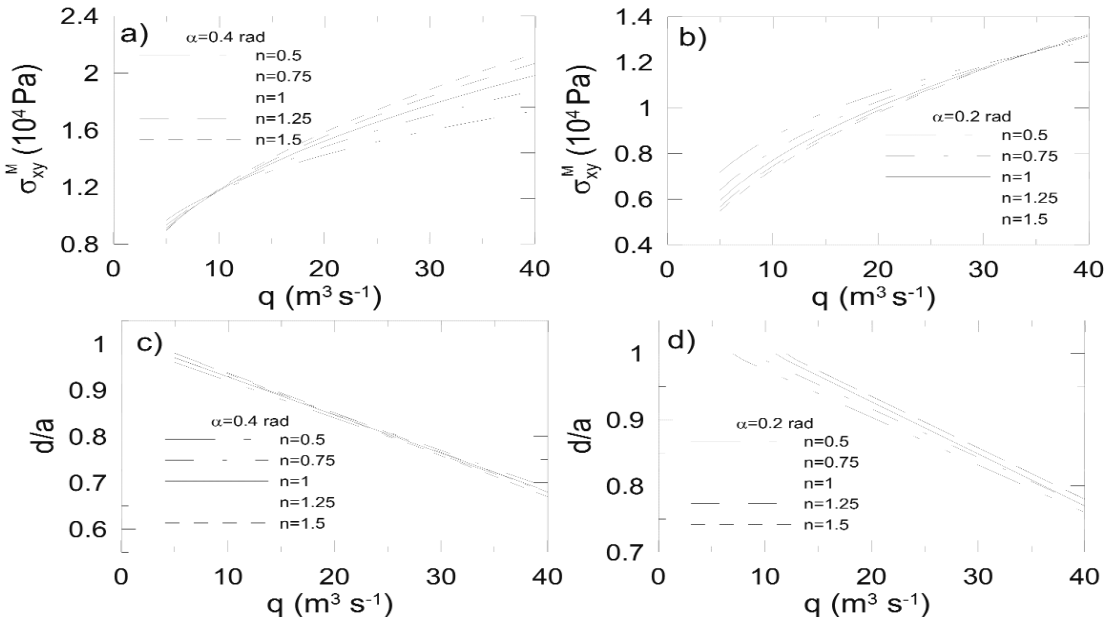

Fig. 6 - $\dot{\sigma}^M_{xy}$ as function of volume flow rate q (a=10 m, ρ=2800 kg m^{-3}, k=10^4 Pa s^n) for α = 0.4 rad (a) and α = 0.2 rad (b); d/a as function of q for α = 0.4 rad (c) and α = 0.2 rad (d).

6). We also found that conditions for tube formation are favoured for thin channels, for gentle slopes and for low volume flow rates. It is worth noting that the use of a power-law rheology in this case does not produce important differences with respect to the Newtonian rheology. The only exception is shown in Fig. 6d, where it can be seen that, for a pseudoplastic fluid, the volume flow rate must be lower than in the case of a Newtonian and a dilatant fluid, in order to achieve the condition for tube formation.

In conclusion, we have shown here that the formation of a lava tube, due to topographic and morphological variations of the lava channel, has a slight dependence on the non-linearity of the fluid and the results of Valerio *et al.* (2008) on the Newtonian fluid seem to be valid also for power-law fluids.

The effect of non-linear rheology is more important when a cooling process is considered. In fact, we have shown that the rapidity of the crust formation, due to a constant heat flow, at the lava channel surface strongly depends on the degree of non-linearity of rheology.

So, although the effect of a power-law rheology can be considered negligible when topographic and morphological variations occur, the power-law rheology plays a very important role when thermal variations occur. Due to the importance of the cooling process of a gravity-driven, lava flow involving the power-law rheology, this matter should be object of more detailed future studies.

Acknowledgements. We thank C. Del Negro for the interesting comments to the manuscript and P. Dellino for the careful reading of the paper. This research has benefited from funding provided by the Italian Presidenza del Consiglio dei Ministri, Dipartimento della Protezione Civile (DPC).

REFERENCES

Bagdassarov N. and Pinkerton H.; 2004: *Transient phenomena in vesicular lava flows based on laboratory experiments with analogue materials*. J. Volcanol. Geotherm. Res., **132**, 115-136.

Capobianchi M.; 2008: *Pressure drop predictions for laminar flows of extended modified power law fluids in rectangular duct*. Int. J. Heat Mass Transfer, **51**, 1393–1401.

Cashman K.V., Kerr R.C. and Griffiths R.W.; 2006: *A laboratory model of surface crust formation and disruption on channelized lava flows*. Bull. Volc., **68**, 753-770.

Champallier R., Bystricky M. and Arbaret L.; 2008: *Experimental investigation of magma rheology at 300 MPa: from pure hydrous melt to 75 vol. \% of crystals*. Earth Planet. Sc. Lett., **267**, 571-583.

Dragoni M., Piombo A. and Tallarico A.; 1995: *A model for the formation of lava tubes by roofing over a channel*. J. Geophys. Res., **100**, 8435– 8447.

Ferziger J.H. and Peric M.; 2002: *Computational methods for fluid dynamics*. Springer-Verlag, Berlin, 423 pp.

Filippucci M., Tallarico A. and Dragoni M.; 2010: *A three dimensional dynamical model for channeled lava flow with non-linear rheology*. J. Geophys. Res., **115**, B05202.

Griffiths R.W., Kerr R.C. and Cashman K.V.; 2003: *Patterns of solidification in channel flows with surface cooling*. Journal of Fluid Mechanics, **469**, 33-62.

Patankar S.V.; 1980: *Numerical heat transfer and fluid flow*. Series in Computational Methods in Mechanics and Thermal Sciences, Taylora Francis, 214 pp.

Peterson D.W., Holcomb R.T., Tilling R.I. and Christiansen R.L.; 1994: *Development of lava tubes in the light of observations at Mauna Ulu, Kilauea Volcano, Hawaii*. Bull. Volcanol., **56**, 343– 360.

Pinkerton H. and Stevenson R.; 1992: *Methods of determining the rheological properties of magmas at sub-solidus temperatures*. J. Volcanol. Geotherm. Res., **53**, 47-66.

Shaw H.R., Wright T.L., Peck D.L. and Okamura R.;1968: *The viscosity of basaltic magma: an analysis of field measurements in Makaopuhi lava lake*, *Hawaii*. Am. J. Sci., **266**, 255-264.

Smith J.V.; 2000: *Textural evidence for dilatant (shear thickening) rheology of magma at high crystal concentrations*. J. Volcanol. Geotherm. Res., **99**, 1–7.

Sonder I., Zimanowski B. and Büttner R.; 2006: *Non-Newtonian viscosity of basaltic magma*. Geoph. Res. Lett., **33**, L02303, doi: 10.1029/2005GL024240.

Spera J., Borgia A., Strimple J. and Feigenson M.; 1988: *Rheology of melts and magmatic suspensions 1. design and calibration of concentric cylinder viscosimeter with application to rhyolitic magma*. J. Geophys. Res., **93**, 10273-10294.

Syrjälä, S.; 1995: *Finite-element analysis of fully developed laminar flow of power-law non-Newtonian fluid in a rectangular duct.* Int. Commun. Heat Mass Transfer, **22**, 4, 549–557.

Valerio A., Tallarico A. and Dragoni M.; 2008: *Mechanisms of formation of lava tubes*. J. Geoph. Res., **113**, B08209, doi: 10.1029/2007JB005435.

Corresponding author: Marilena Filipucci
Istituto Nazionale di Geofisica e Vulcanologia, Sez. di Catania
Piazza Roma, 2, 95152 Catania, Italy
Phone: +39 080 5742419; e-mail: filippucci@ct.ingv.it